Proceedings of the 8th World Congress on Electrical Engineering and Computer Systems and Sciences (EECSS'22)
Prague, Czech Republic - July 28- 30, 2022
Paper No. EEE 112
DOI: 10.11159/eee22.112

An LLC Resonant Converter with Double Resonant Tanks for Wide-Input-Voltage-Range Applications

Ezekiel Bokolonga[1], Yao-Ching Hsieh[2], David Welchman Gegeo[1]
[1]Department of Electrical Engineering, Solomon Islands National University
Kukum Campus, Honiara, Solomon Islands
ezekiel.bokolonga@sinu.edu.sb; david.gegeo@sinu.edu.sb
[2]Department of Electrical Engineering, National Sun Yat-Sen University
70 Lienhai Rd., Kaohsiung 80424, Taiwan
ychsieh@mail.ee.nsysu.edu.tw

Abstract **-** This paper presents an LLC resonant converter with double resonant tanks configured for a wide-input-voltage range application. The converter comprises four power switches (MOSFETs), a pair of resonant tanks with LLC configuration, and two centre-tapped transformers. Its operation is similar to that of a conventional half-bridge LLC resonant converter, where the primary windings of the transformers are connected across the half-bridge network via the tanks. However, the main attributing factor to the design is the ability to operate in two consecutive modes, depending on the desired input voltage range. Mode 1 is operational to a low input voltage range while Mode 2 is operational to a high input voltage range. These two modes delivered power twice every cycle to the load in a different fashion (switching techniques) but with the same ability to share power among the resonant tank elements for voltage/current stress relieve. Interestingly, each mode regulates the output for a wide input voltage range within the same frequency range. The operation and analysis of the proposed converter is respectively discussed in this paper followed by a validation with experimental results.

Keywords**:** LLC resonant converter, double resonant tanks, wide-input-voltage-range, soft-switching.

1. Introduction

There have been numerous research studies conducted on various types of power converter design nowadays which can achieve quite a variety of applications. Traditional and conventional converters are the building blocks of all these adventures. However, the major issue encountered with traditional and conventional converters is the ability to achieve soft switching, and this makes it difficult to meet the growing demand of high-power density and simplicity. The evolution of resonant converters however gives researchers an opportunity to address the issue of hard switching and develop other interesting features that provide strength for future converter designs.

Resonant converters in recent years have become more popular and widely used due to the following key features: (1) it can achieve Zero Voltage Switching (ZVS) and Zero Current Switching (ZCS), both of which can perform the features of soft-switching, which can reduce switching losses; (2) it can operate at higher frequencies, reducing the size of passive components used; (3) it can achieve and maintain high efficiency over wide line and load variations.

Different from pulse width modulation (PWM) converters, resonant converters rely on frequency modulation (FM) to regulate its output. With a fixed duty cycle, changing the frequency of the converter also changes the impedance of the resonant network. This helps to observe the gain in a wider range, depending on the type of configuration used. The two basic configurations possible for a load connection are series and parallel connections. These two configurations however have limitations which are related to their operation. A remedy to these limitations is the hybrid configuration, which is the combination of both series and parallel connections. Under hybrid configuration are the two most commonly known LCC and LLC resonant converters, both portraying the likes of series resonant converter (SRC) and parallel resonant converter (PRC) [1].

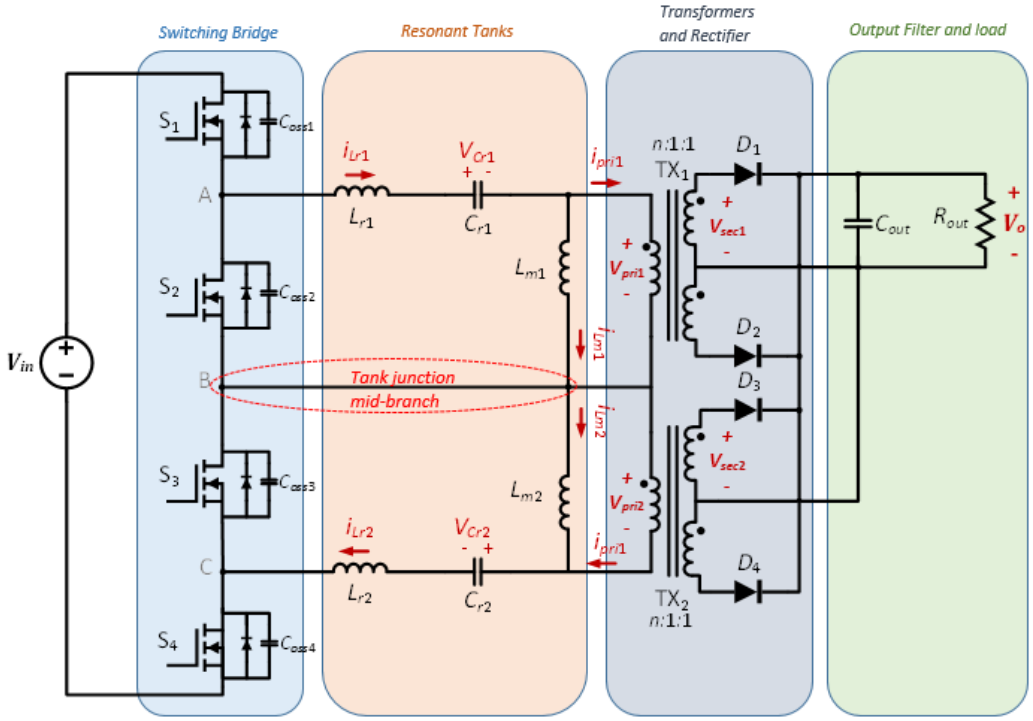

Fig. 1: Schematic of proposed converter.

LCC and LLC type resonant converters solve the issue depicted by series and parallel configurations, however, both can still portray important drawbacks. Since an optimized design for a resonant converter normally operates close-to/at the resonant frequency, varying the input voltage also varies the switching frequency, which gives the LCC topology a bad situation when operating at high input voltage. LCC type converter therefore not suitable for this condition since its efficiency degrades due to conduction and switching losses. With this drawback, LLC resonant converter gains the interest and is featured in most recent studies in several different types of configurations, ranging from full-bridge, half-bridge, interleaved, three-level and double resonant tanks [2] - [9].

Over wide line and load variations, LLC resonant converter regulates its output relatively with small variation of the switching frequency. However, since LLC resonant converter generally focuses on two regions of operation (inductive and capacitive regions), there are limitations to its design [10], [11]. Considering this design limitations, an analysis of the worst-case operation is needed. The worst-case operation for any LLC type configuration occurs when the converter operates over a wide input voltage range, and even worsen when the input voltage is at its minimum.

Since most application nowadays requires a wider range of input voltage, this paper aims to develop a resonant converter, that portraits the likes of a double resonant tanks and could operate efficiently over a wide-input-voltage-range without being influenced by the design limitations.

This paper contains five sections. Section 1 is on development and motivation of research topic. Section 2 reviews the basic circuit operation and analysis in steady state. Section 3 describes the gain characteristics of the proposed converter. Section 4 validates the analysis with experimental results. Section 5 summarizes the proposed design.

2. Circuit Operation and Analysis in Steady State

Fig. 1 shows the basic configuration of the proposed converter. Different from the conventional half bridge LLC resonant converter, the proposed converter is implemented in two modes. Mode 1 is operational for low input voltage range and Mode 2 is operational for high input voltage range. Each mode has eight operating intervals, with the same frequency range for regulating the output voltage. This section describes the operation of both modes.

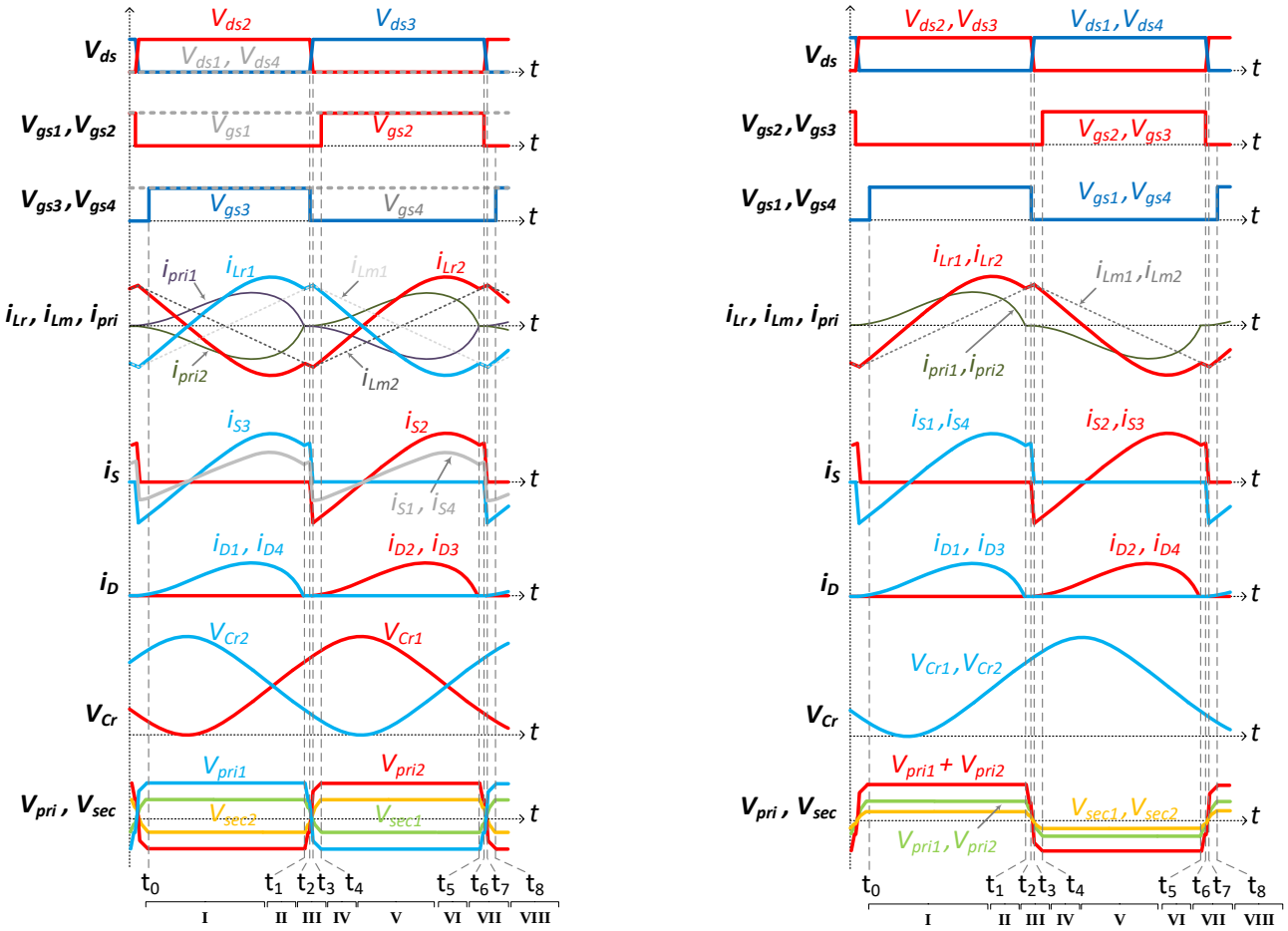

(a) Mode 1 (b) Mode 2

Fig. 2: Key steady state operating waveforms.

Fig. 2 shows the key waveforms of the proposed converter in steady state operation for both modes. Referring to Fig. 2(a), Mode 1 operates in the following fashion: Switches S_1 and S_4 are driven with 100% duty ratio, turning ON for the entire cycle. Switching is only done between switches S_2 and S_3, driven with approximately 50% duty ratio in complement with each other. Referring to Fig. 2(b), Mode 2 operates in the following fashion: Switches S_1 and S_4 are driven in complement to switches S_2 and S_3 with approximately 50% duty ratio respectively. The analysis for either mode is based on the first four intervals, whose operating circuits are respectively shown in Figs. 3 and 4. To simplify the analysis, several assumptions are made:

1) All switches are MOSFETS with equal output capacitors (C_{oss}).
2) Resonant tanks element are equal respectively.
   i.e., $L_r = L_{r1} = L_{r2}$, $C_r = C_{r1} = C_{r2}$, $L_m = L_{m1} = L_{m2}$
3) Both transformers are identical with same turn's ratios.
   i.e., $n = N_p/N_s$
   where, $N_p = N_{p1} = N_{p2}$
   $N_s = N_{s1} = N_{s2}$
4) The output capacitor C_{out} is large enough to supply the load during a switching period.
5) All secondary side rectifier diodes are perfectly coupled during operation.
6) No current is flowing through the "tank junction mid-branch (*see* Fig. 1)" during Mode 2 operation.

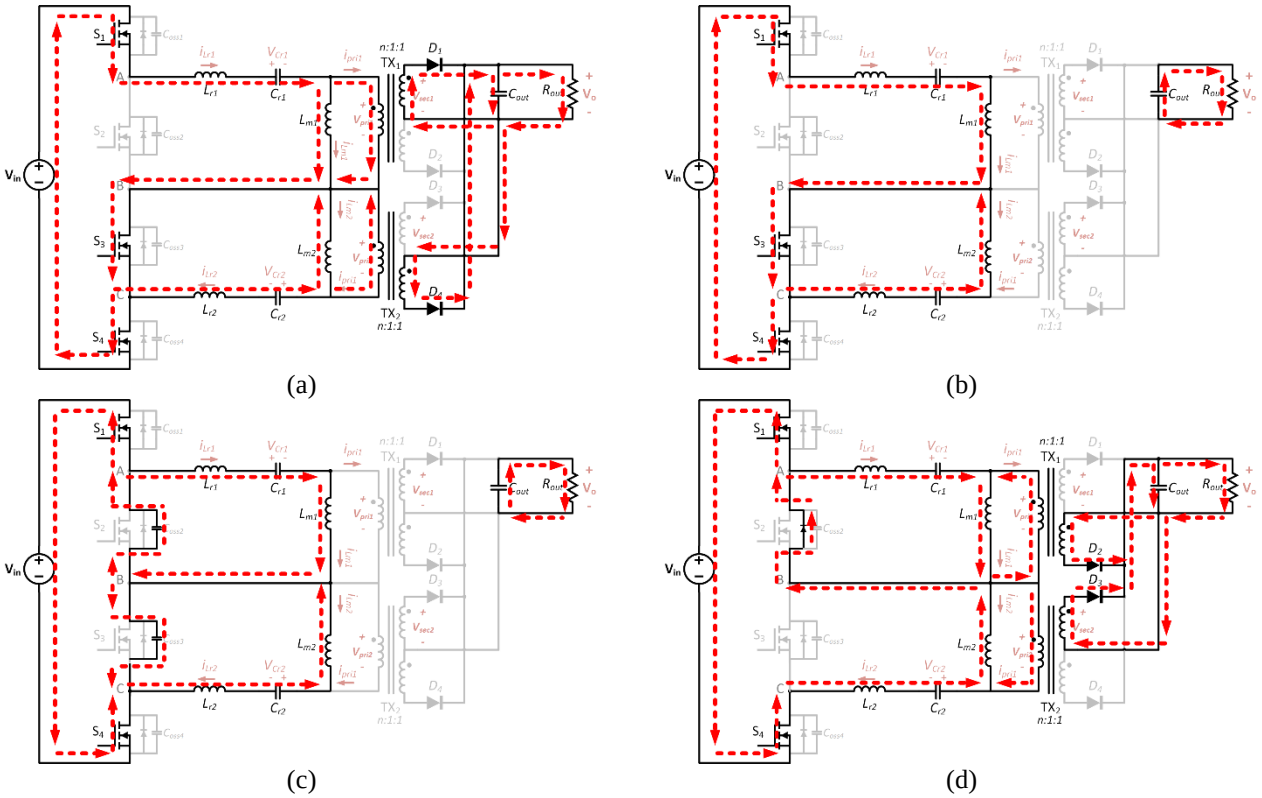

Fig. 3: Mode 1 operating circuits of the proposed converter: (a) Mode 1-I; (b) Mode 1-II; (c) Mode 1-III; (d) Mode 1-IV.

2.1. Mode 1 Steady State Analysis

Mode 1-I [$t_0 – t_1$]: This interval begins at time t_0. Prior to this time, body diode of switch S_3 conducts, allowing S_3 to turn on with ZVS. Input terminals A and B connected across the input voltage source, delivering the input power to the load via tank 1 (L_{r1}, C_{r1}, L_{m1}). During this same interval, input terminals B and C of tank 2 (L_{r2}, C_{r2}, L_{m2}) are shorted by switch S_3, thus tank 2 transferred its previously stored power to the output. This gives the sinusoidal swing of resonant currents i_{Lr1} and i_{Lr2} in opposite directions respectively. The resonant capacitors (C_{r1} and C_{r2}) in response charges and discharges. On the secondary sides of transformers TX_1 and TX_2, rectifier diodes D_1 and D_4 conducts, reflecting the output voltage to the primary sides, giving the linear rise and fall slopes (nV_o/L_{m1} and $–nV_o/L_{m2}$) of magnetizing currents i_{Lm1} and i_{Lm2} respectively. This interval ends with magnetizing and resonant currents equal to each other at t_1, leaving D_1 and D_4 reverse biased. Therefore, both diodes turned off respectively.

Mode 1-II [$t_1 – t_2$]: Interval II starts off with magnetizing currents (i_{Lm1} and i_{Lm2}) and resonant currents (i_{Lr1} and i_{Lr2}) equal to each other at time t_1. Since D_1 and D_4 are reverse biased, both turned off respectively with ZCS. This interval involves the magnetizing inductors (L_{m1} and L_{m2}) to resonate with the resonant elements (L_{r1}, C_{r1}, L_{r2}, *and* C_{r2}). Secondary sides of transformers TX_1 and TX_2 are isolated from the primary sides, thus, the output capacitor C_{out} supplied power to the load. This interval ends with turning-off of switch S_3 at t_2,where resonant currents discharges and charges the output capacitors of switches S_2 and S_3 (C_{oss2} and C_{oss3}) respectively.

Mode 1-III [$t_2 – t_3$]: This interval starts with switch S_3 turns off at t_2. The output capacitors of switches S_3 and S_2 (C_{oss3} and C_{oss2}) charges and discharges approximately to input voltage and zero, which done by the resonant currents respectively. It is also during this interval that the output power is being offered independently by the output capacitor, C_{out}.

Mode 1-IV [$t_3 – t_4$]: Interval IV begins at time t_3. Prior to this time, output capacitors of switches S_3 and S_2 (C_{oss3} and C_{oss2}) charges and discharges approximately to input voltage and zero completely, forward biased the body diode of switch S_2. This allows the resonant current to turn on switch S_2 with ZVS in the next half cycle. Input terminals A and B of tank 1

are shorted to the input voltage source, thus, tank 1 delivers its previous stored power to the output, while tank 2 transfers power from the input source to the load due to its input terminals B and C being connected across the input voltage source. Resonant currents and voltages (i_{Lr1}, i_{Lr2}, V_{Cr1}, V_{Cr2}) in respond are similar to what is described earlier in interval I. Secondary side rectifier diodes D_2 and D_3 conducts, clamping the primary sides of transformers TX_1 and TX_2 to the output voltage ($-nV_o$ and nV_o). This gives the linear fall and rise slopes ($-nV_o/L_{m1}$ and nV_o/L_{m2}) of magnetizing currents i_{Lm1} and i_{Lm2}. This interval ends with switch S_2 turns on with ZVS at t_4.

2.2. Mode 2 Steady State Analysis

Mode 2-I [$t_0 - t_1$]: This interval begins at time t_0. Prior to that time, body diode of switches S_1 and S_4 conducts, allowing both switches to turn on with ZVS at time t_0. Input terminals A and C (L_{r1}, C_{r1}, L_{m1}, L_{r2}, C_{r2}, L_{m2}) connects across the input voltage source, allowing power to transfer from input to output via both the tanks simultaneously. This gives the sinusoidal swing of resonant currents i_{Lr1} and i_{Lr2} in the same direction, charging both the resonant capacitors (C_{r1} and C_{r2}) simultaneously. At this interval, secondary side rectifier diodes D_1 and D_3 conducts, clamping the primary sides of transformers TX_1 and TX_2 to the output voltage, which gives the linear rising slope (nV_o/L_{m1} and nV_o/L_{m2}) of the magnetizing currents i_{Lm1} and i_{Lm2}. This interval ends at t_1, when the magnetizing and resonant currents equal to each other. At this saturation, D_1 and D_3 both reverse biased, therefore turned off respectively.

Mode 2-II [$t_1 - t_2$]: This interval starts with magnetizing currents (i_{Lm1} and i_{Lm2}) equal to the resonant currents (i_{Lr1} and i_{Lr2}) at t_1. Diodes D_1 and D_3 on the secondary side both reverse biased, therefore turned off respectively with ZCS. Both magnetizing inductors (L_{m1} and L_{m2}) involved in resonance with the resonant elements (L_{r1}, C_{r1}, L_{r2}, *and* C_{r2}), leaving the secondary side isolated from the primary side. It is the output capacitor C_{out} that supplied power to the load. This interval ends with switches S_1 and S_4 turns off at t_2, allowing resonant currents to discharge and charge both the output capacitors of switches S_2 and S_3 (C_{oss2} and C_{oss3}) and switches S_1 and S_4 (C_{oss1} and C_{oss4}).

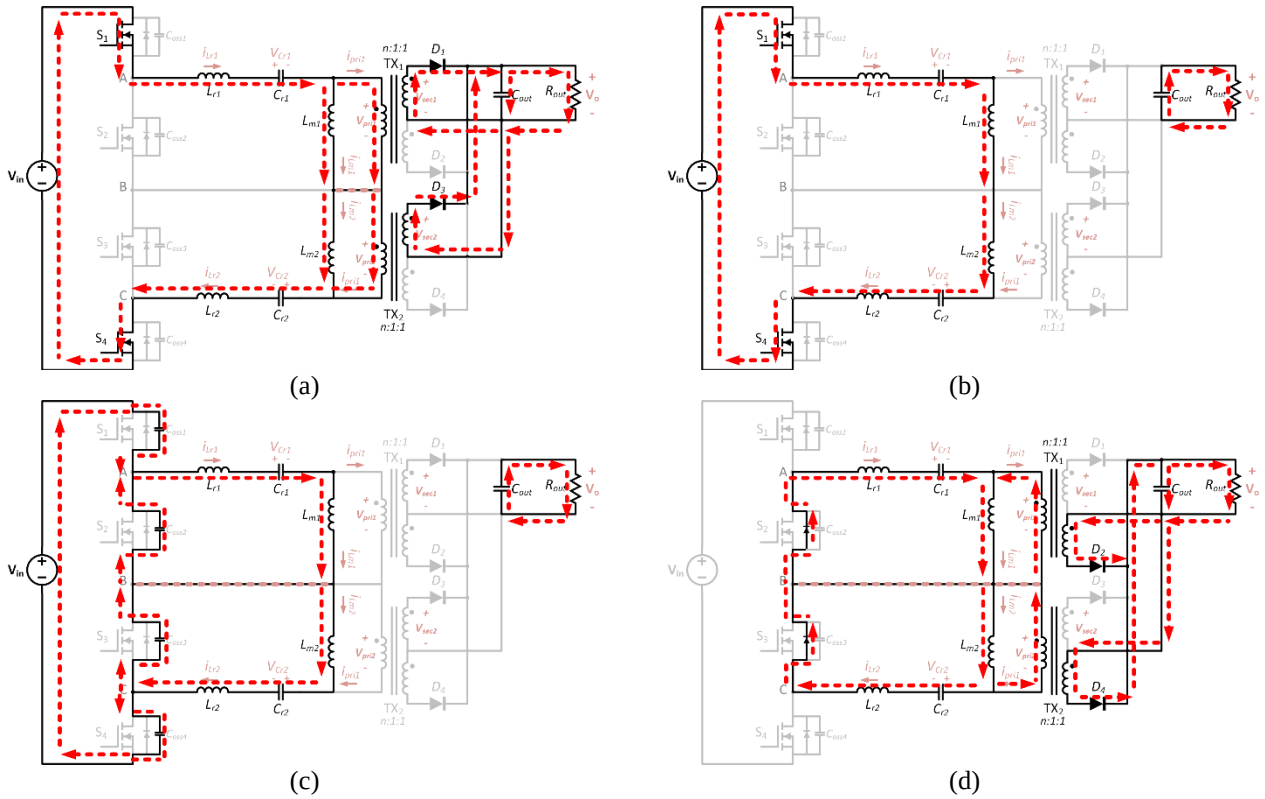

Fig. 4: Mode 2 operating circuits of the proposed converter: (a) Mode 2-I; (b) Mode 2-II; (c) Mode 2-III; (d) Mode 2-IV.

Mode 2-III [$t_2 - t_3$]: Interval III starts with switches S_1 and S_4 turns off at t_2. The output capacitors of switches S_2 and S_3 (C_{oss2} and C_{oss3}) and switches S_1 and S_4 (C_{oss1} and C_{oss4}) discharges and charges approximately to zero and the input voltage.

Mode 2-IV [$t_3 - t_4$]: This interval starts at time t_3 prior to the output capacitors of switches S_1 and S_4 (C_{oss1} and C_{oss4}) and switches S_2 and S_3 (C_{oss3} and C_{oss2}) being completely charged and discharged approximately to input voltage and zero. Body diodes of switches S_2 and S_3 are forward biased, allowing the current to resonate through them in order to turn on with ZVS in later mode. The input terminals A and C are shorted and floating, delivering the previous stored energy of both tanks to the output via D_2 and D_4. The respond of resonant currents and voltages (i_{Lr1}, i_{Lr2}, V_{Cr1}, V_{Cr2}) are similar to what is described in mode 2-I. Secondary side rectifier diodes D_2 and D_4 clamps the primary sides to the output voltage ($-nV_o$), which leads to linear falling slopes ($-nV_o/L_{m1}$ and $-nV_o/L_{m2}$) of magnetizing currents i_{Lm1} and i_{Lm2}. This interval ends with switches S_2 and S_3 turn on with ZVS at t_4.

Because of symmetrical operation, intervals V to VIII of both modes are not described in this paper, however, it can be obtained in similar manner to intervals I to IV. Another important note is when the switching and resonant frequency are equal, the operation of the proposed converter in both the modes is minimized into six intervals. However, this is practically not attainable.

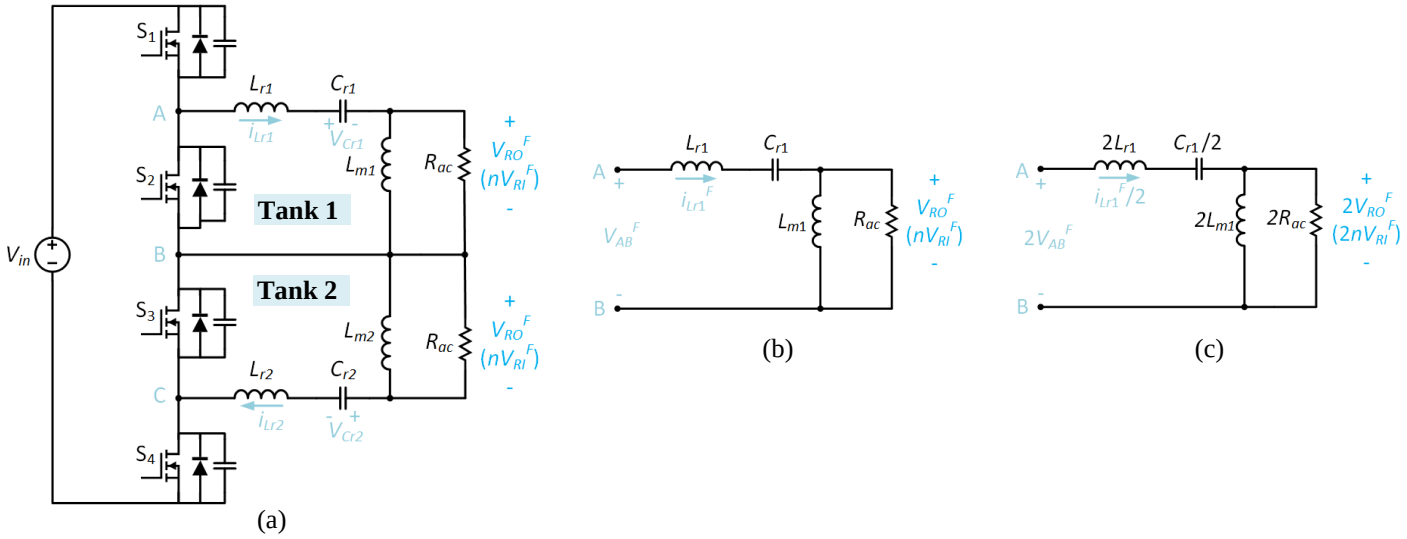

Fig. 5: (a) Equivalent circuit with AC load. (b) Mode 1 AC equivalent circuit. (c) Mode 2 AC equivalent circuit.

3. Gain Characteristics of the Proposed Converter

To analyze the characteristic of the converter, it is preferable to simplify the circuit into its AC equivalent form as shown in Fig. 5, from which the gain of the converter can be obtained. The basic method used to obtain such equivalent circuit is known as the Fundamental Harmonics Approximation (FHA) [12], [13]. This method accompanies only the fundamental components of both current and voltage, neglecting other additional influences that might be valuable for other means of interest. Using this approach, the output resistor R_{out} of the converter (*see* Fig. 1) is reflected to the primary side as an equivalent resistor R_{ac} (*see* Fig. 5). Fig. 5(a) shows the equivalent circuit of the design when R_{out} is reflected to the primary sides of both transformers TX_1 and TX_2 in Fig. 1 as R_{ac}'s. Extracted from Fig. 5(a) are the AC equivalent circuits used for Modes 1 (Fig. 5(b)) and 2 (Fig. 5(c)) analysis. For Mode 1, the gain characteristics of both tanks in Fig. 5(a) are similar; therefore, it is reasonable to do evaluation only on a single tank circuit, as shown in Fig. 5(b). For Mode 2, the gain characteristics of tanks 1 and 2 in Fig. 5(a) are added, thus, by assuming the gain characteristics of both tanks are similar, it is also reasonable to do evaluation on a single tank circuit by doubling the values of either of the tanks, as shown in Fig. 5(c). Using the ac equivalent circuits in Fig. 5(b and c), assuming the evaluation is done on tank 1 (L_{r1}, C_{r1}, L_{m1}, and TX_1), the following expression for gain M is derived for each mode as;

$$\text{Mode 1: } M = 2n\frac{V_o}{V_{in}} = \frac{k}{\sqrt{\left(1+k-\frac{1}{f_n^2}\right)^2 + Q^2k^2\left(f_n-\frac{1}{f_n}\right)^2}} \tag{1}$$

$$\text{where } \begin{cases} k = \dfrac{L_{m1}}{L_{r1}}, \quad Q = \dfrac{\sqrt{L_{r1}/C_{r1}}}{R_{ac}} \quad for\ R_{ac} = \dfrac{8n^2R_{out}}{\pi^2} \\ n = \dfrac{N_p}{N_s}, \quad f_n = \dfrac{f_{sw}}{f_r} \quad for\ f_r = \dfrac{1}{2\pi\sqrt{L_{r1}C_{r1}}} \end{cases}$$

$$\text{Mode 2: } M = 4n\frac{V_o}{V_{in}} = \frac{k}{\sqrt{\left(1+k-\frac{1}{f_n^2}\right)^2 + Q^2k^2\left(f_n-\frac{1}{f_n}\right)^2}} \tag{2}$$

$$\text{where } \begin{cases} k = \dfrac{2L_{m1}}{2L_{r1}}, \quad Q = \dfrac{\sqrt{2L_{r1}\Big/(\frac{1}{2}C_{r1})}}{R_{ac}} \quad for\ R_{ac} = \dfrac{16n^2R_{out}}{\pi^2} \\ n = \dfrac{2N_p}{2N_s}, \quad f_n = \dfrac{f_{sw}}{f_r} \quad for\ f_r = \dfrac{1}{2\pi\sqrt{2L_{r1}(\frac{1}{2}C_{r1})}} \end{cases}$$

In the circuit definitions for (1) and (2), the equivalent resistance R_{ac} used in Modes 1 and 2 analyses are different, however the value of Q obtained for each mode is the same due to the characteristic impedance of the resonant tank changes with respect to each mode of operation. The turn's ratio n (N_p/N_s) of the transformers remains the same in either of the modes.

Table 1: Component list.

Input voltage	Mode 1: 115 V and Mode 2: 230 V
Output voltage	35 V
Input capacitor (C_{in})	100 µF
Resonant frequency (f_r)	116 kHz
Switching frequency (f_{sw})	110 kHz
Primary switches (S_1, S_2, S_3, S_4)	SCT3030AL (V_{DSS}: 650 V, $R_{DS(on)}$: 30 mΩ)
Secondary diodes (D_1, D_2, D_3, D_4)	HFA15TB60 (V_R: 600 V, V_F: 1.7 V)
Resonant inductances (L_{r1}, L_{r2})	12 µH
Resonant capacitances (C_{r1}, C_{r2})	156 nF/680 V
Magnetizing inductances (L_{m1}, L_{m2})	22 µH
Transformer turns ratio ($n = N_p/N_s = 2$) N_{p1}:N_{s1}:N_{s2} N_{p2}:N_{s1}:N_{s2}	 18 : 9 : 9 18 : 9 : 9
Output capacitor (C_{out})	660 µF
Output power (P_{out} @ *full-load*)	255 W

4. Experimental Results

The performance and operating principles of the proposed converter was verified by a 480 W prototype using the components shown in Table 1. A switching frequency of 110 kHz was used to regulate the output voltage at 35 V, with a fixed duty ratio of 50% on each respective switches, depending on the type of mode used. Combining the input voltages specified in *table 1* for each mode gives the input voltage range of 115 – 230 V for the experiment. This proves the ability of the overall design to operate at an input voltage range of 115 – 460 V, with nominal inputs of 190V and 380V for Modes 1 and 2. Due to limitation of DC input power supply, the prototype was tested only for 115 V (Mode 1) and 230 V (Mode 2) input voltages, giving an output power of 255 W. However, these two inputs provide enough information to validate the design specification. Note that for the overall design, Modes 1 and 2 minimum input voltages are 115 V and 230 V, which is also the voltage levels used in the experiment for each respective mode. Fig. 6 and 7 depicts the key steady state experimental waveforms obtained for the two input voltage levels.

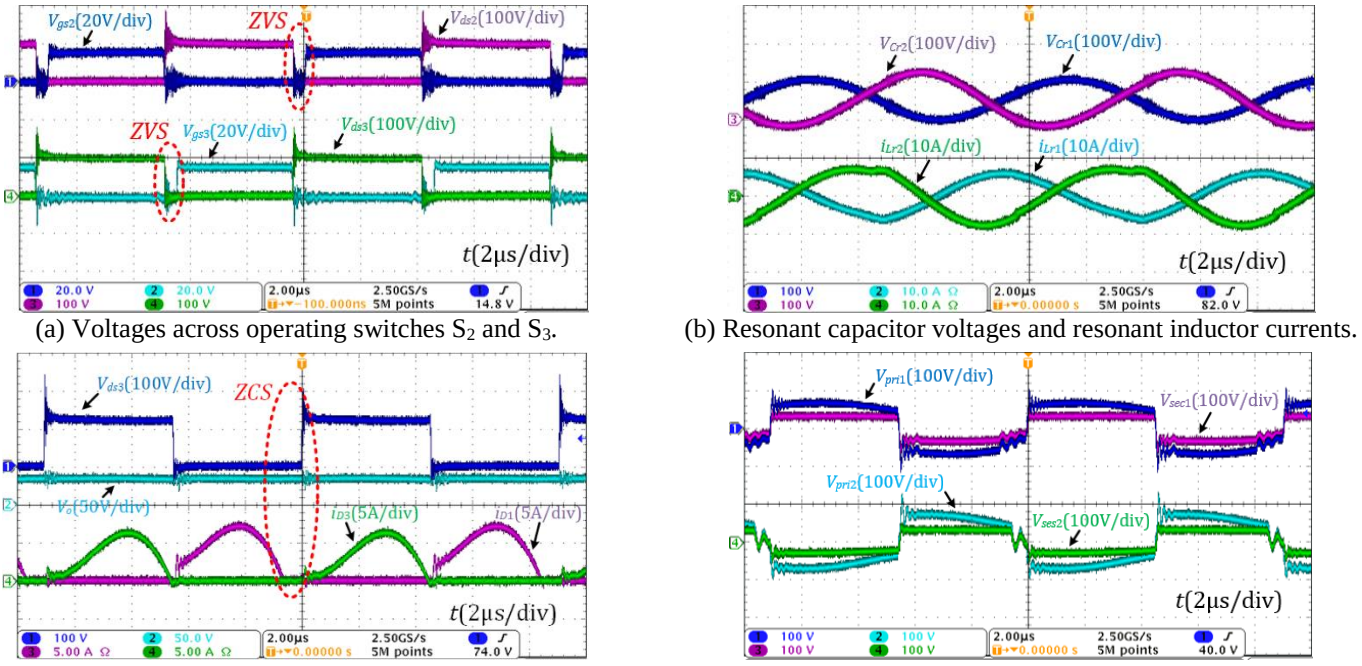

(a) Voltages across operating switches S_2 and S_3.

(b) Resonant capacitor voltages and resonant inductor currents.

(c) Voltage across operating switch S_3, output and the rectifier diode currents.

(d) Primary and secondary voltages of the transformers.

Fig. 6: Key steady state experimental waveforms for Mode 1 voltage.

Fig. 6 shows the key steady state experimental waveforms of Mode 1 voltage. By looking at the waveforms in Fig. 6(a), S_2 and S_3 operate under ZVS condition. Fig. 6(b) shows the waveforms of resonant voltage and current of capacitors (C_{r1} and C_{r2}) and inductors (L_{r1} and L_{r2}) of the resonant tanks. The waveforms illustrate the sinusoidal swing of resonant currents i_{Lr1} and i_{Lr2} in opposite directions respectively. This indicates the charging and discharging of resonant capacitors, which depicts the distribution of power twice every cycle to the output. The resonating behaviour of these waveforms are expected to be symmetrical but due to the resonant components miss-matched, the amplitudes and phases are not identical. In response, the waveforms of the rectifier diode currents in the secondary side are not perfectly coupled, as shown in Fig. 6(c). However, the secondary diodes conducted in expected combination. The drain-source voltage of switch S_3 and diode current i_{D1} are compared in Fig. 6(c) to show that ZCS of i_{D1} has been achieved. Fig. 6(d) shows the primary and secondary voltages of transformers TX_1 and TX_2. From the waveforms, opposite rise and fall of the voltages have been obtained respectively with the secondary side voltages being scaled down by approximately 2 for both primary voltages. With the output voltage of 35 V, the maximum efficiency of the converter for Mode 1 is 96.99%.

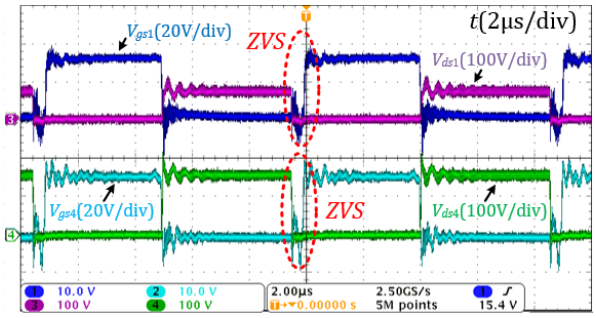

(a) Voltages across operating switches S_1 and S_4.

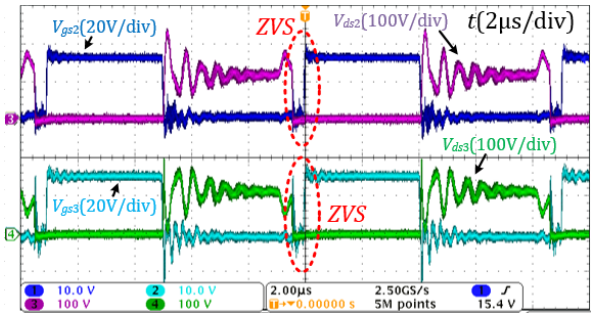

(b) Voltages across operating switches S_2 and S_3.

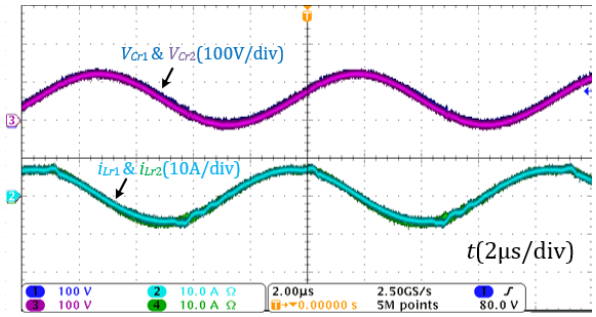

(c) Resonant capacitor voltages and resonant inductor currents.

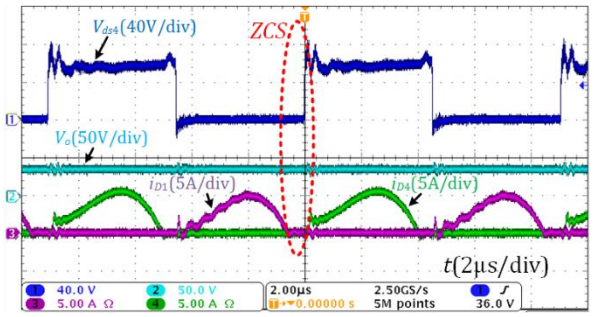

(d) Voltage across operating switch S_4, output and the rectifier diode currents.

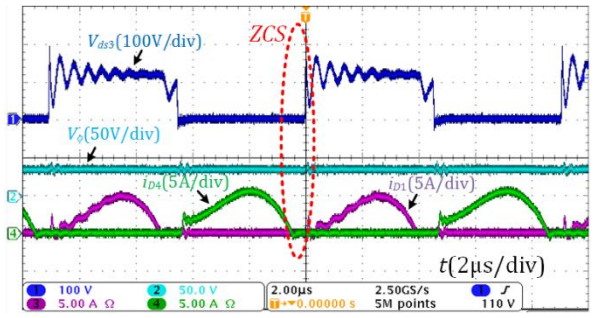

(e) Voltage across operating switch S_3, output and the rectifier diode currents.

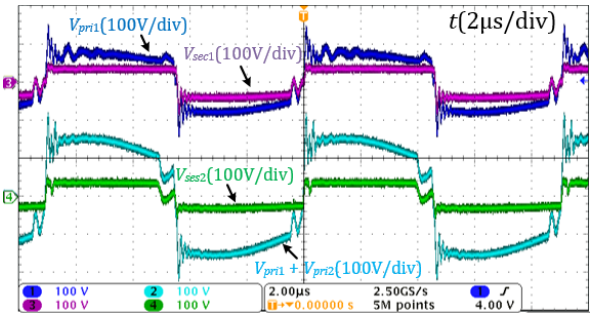

(f) Primary and secondary voltages of the transformers.

Fig. 7: Key steady state experimental waveforms for Mode 2 voltage.

Fig. 7 shows the key steady state experimental waveforms of Mode 2 voltage. As shown in the waveforms of Fig. 7(a) and Fig. 7(b), S_1, S_2, S_3 and S_4 operate under ZVS condition. However, from Fig. 7(b), there is ringing on V_{ds2} and V_{ds3} due to the output capacitances of S_2 and S_3 being resonating with the parasitic inductances of the circuit, which also affects V_{ds1} and V_{ds4} being unbalanced. Fig. 7(c) shows the waveforms of resonant voltage and current of capacitors (C_{r1} and C_{r2}) and inductors (L_{r1} and L_{r2}) of both respective tanks. The waveforms illustrate the sinusoidal swing of resonant currents i_{Lr1} and i_{Lr2} in the same direction respectively. This indicates simultaneous charging and discharging of resonant capacitors, which depicts the distribution of power twice every cycle to the load. The resonating behaviour of these waveforms is almost symmetrical, which illustrates balancing mechanism of the converter. In response, the waveforms of the rectifier diode currents in Fig. 7(d) and Fig. 7(e) are likely to be coupled and conducted in expected combination. The drain-source voltage of switches S_3 and S_4 are compared with diode currents i_{D1} and i_{D4} to illustrate the effect of ZCS. Fig. 7(f) shows the primary and secondary voltages of transformers TX_1 and TX_2. From the waveforms, simultaneous rise and fall of the voltages have been obtained respectively with the secondary side voltages being scaled down by approximately 2 for V_{pri1} and

approximately 4 for $V_{pri1} + V_{pri2}$. With the output voltage of 35V in Fig. 7(d & e), the maximum efficiency of the converter for Mode 2 is 97.85%.

5. Conclusion

A proposed LLC resonant converter with double resonant tanks was presented in this paper. Its operating principle was analyzed based on its steady state form. The converter was designed to operate efficiently in a wide-input-voltage-range and was verified with experimental results in Section 4. A 480W prototype with input voltage ranges of 115-460V was designed to achieve 48V output voltage under a full-load (10A) condition. This was achieved by two modes of circuit operation, operating in the same frequency range, with specified input voltage ranges. Due to limitation of DC input power supply, the prototype was implemented and tested only with two input voltage levels of 115V and 230V, specified for each mode. Each mode was tested respectively and gives the output voltage and power of 35 V and 255 W. The experiment proves that the converter can regulate its output voltage over a specified frequency range with corresponding input voltage levels for each respective mode. This proposed converter is vital for wide-input-voltage-range applications and can be explored if additional improvements are needed.

Acknowledgement

This work was supported by the Ministry of Science and Technology, Taiwan, under Grant 107-2218-E006-003-.

References

[1] H. Choi, "Design Considerations for an LLC Resonant Converter," in *Fairchild Semiconductor*, Bucheon-si, 2007.

[2] I.-O. Lee, S.-Y. Cho and G.-W. Moon, "Three-Level Resonant Converter With Double LLC Resonant Tanks for High-Input-Voltage Applications," *IEEE TRANSACTIONS ON INDUSTRIAL ELECTRONICS*, vol. 59, no. 9, p. 14, 2012.

[3] Y. Gu, Z. Lu, L. Hang, Z. Qian and G. Huang, "Three-Level LLC Series Resonant DC/DC Converter," *IEEE TRANSACTIONS ON POWER ELECTRONICS*, vol. 20, no. 4, p. 9, 2005.

[4] S. Iqbal, "Double Resonant Tanks Based DC-DC Converter with Integrated Dual Transformers for PV Power Systems," in *IEEE*, Nibong Tebal, 2016.

[5] Texas Instruments, "Designing an LLC Resonant Half-Bridge Power Converter," in *Power Supply Design Seminar*, Dallas, 2011.

[6] S. Abdel-Rahman, "Resonant LLC Converter: Operation and Design," Infineon Technologies, Durham, 2012.

[7] STMicroelectronics, "An introduction to LLC resonant half-bridge converter," STMicroelectronics, Geneva, 2008.

[8] S. D. Simone, "LLC resonant half-bridge converter design guideline," STMicroelectronics, Geneva, 2014.

[9] A. Lind and I. PMM, "LLC Converter Design Note," Infineon Technologies, Villach, 2013.

[10] B. Lu, W. Liu, Y. Liang, F. C. Lee and J. D. v. Wyk, "Optimal Design Methodology for LLC Resonant Converter," in *IEEE*, Blacksburg, 2006.

[11] J.-h. Jung and J.-g. Kwon, "Theoretical Analysis and Optimal Design of LLC Resonant Converter," in *SAMSUNG Electronics Co.*, Suwon-si.

[12] Texas Instruments, "Survey of Resonant Converter Topologies," in *Power Supply Design Seminar*, Dallas, 2018.

[13] X. Zhang, W. You, W. Yao, S. Chen and Z. Lu, "An Improved Design Method of LLC Resonant Converter," in *IEEE*, Hangzhou, 2012.